Available online at www.sciencedirect.com
ScienceDirect
Optics and Lasers in Engineering 45 (2007) 431–441
OPTICS and LASERS in ENGINEERING

Automatic fringe analysis of two-beam interference patterns for measurement of refractive index and birefringence profiles of fibres

T.Z.N. Sokkar[a], H.M. El Dessouky[a,*,1], M.A. Shams-Eldin[b], M.A. El-Morsy[b]

[a]Physics Department, Faculty of Science, Mansoura University, Mansoura 35516, Egypt
[b]Physics Department, Faculty of Science Demietta, Mansoura University, New Demietta, Egypt

Received 1 October 2005; received in revised form 1 August 2006; accepted 1 September 2006
Available online 3 November 2006

Abstract

Automatic fringe pattern analysis is a powerful and inexpensive digital image-processing technique. Two-beam polarizing interference Pluta microscope [Pluta M. Opt Acta 1971;18:661, Pluta M. J Microsc 1972;96:309] is automated by the computer-aid via CCD camera and digital frame grabber. Software program is prepared to deal with the duplicated (separated and overlapped) Microinterferograms produced by two-beam polarizing microscope. It also gives an accurate and fast automatic measurement of refractive index and birefringence profiles for fibres. In this paper, the refractive index and birefringence profiles of two different types of fibres, basalt and polypropylene (PP) fibres are presented. A new method to determine the birefringence profile of fibres from non-duplicated microinterferogram is suggested. The cold drawing process for PP fibres is studied.

Keywords: Interference; Image analysis; Refractive index; Birefringence profiles; Drawing and fibres

1. Introduction

Nowadays, the intensive progress in development of laser sources and optical elements has challenged scientists to use the interferometry as an important diagnostic tool for accurate and gross field measurements of various phenomena. These challenges have resulted in an accurate measurement in almost all engineering domains. For example in chemical engineering, materials science and physical fields, refractive index measurement is frequently needed.

All of interferometric techniques are based on the wave characteristics of light, when it reflects from or transmits through an object. Light transmission properties through a fibre depend mainly on its refractive index profile and material dispersion. In other words, the direct result of an interferometric technique is generally fringe pattern or interferogram. This interferogram provides us with rich quantitative information regarding sample material behaviour.

In the past, the interferograms obtained from the conventional interferometric techniques must be photographed and enlarged to a suitable magnification than the required data are obtained from the magnified image [3–11]. The manual quantitative analysis process is time consuming and very tedious, and furthermore it cannot make a full use of the interferogram's data. For this reason, an automatic image processing of these interferograms is an active topic in recent literatures.

The values of birefringence and refractive indices of fibres for plane polarized light vibrating parallel or perpendicular to the fibre axis are important not only in assessing the performance of the fibre in a given system but also it help in fibres fabrication to improve their products. Therefore, there is an increasing need for fast and accurate measurements of refractive index profile of fibres because it provides information for the correlation between their structure and the other properties.

Usually, the synthetic fibres are manufactured with no desirable tensile properties and low birefringence. In order to turn into useful textile fibres, they must be mechanically

*Corresponding author. Tel.: +4401132172952; fax: +4401133433704.
E-mail address: hassanoptics@yahoo.com (H.M. El Dessouky).
[1]Current address: Department of Textile Industries, University of Leeds, Leeds LS2 9JT, UK.

0143-8166/$ - see front matter © 2006 Elsevier Ltd. All rights reserved.
doi:10.1016/j.optlaseng.2006.09.003

drawn out to make them thinner, stronger and consequently more birefringent. The birefringence of fibres provides valuable information for the correlation between their structural and physical properties. Accordingly these fibres can be classified (based on the value of their birefringence) into three categories, namely; zero (isotropic), low, and high birefringence [12].

Automated, high-speed image processing techniques are used to analyse the fringe pattern and give an accurate analysis. The main procedure in automatic fringe pattern analysis is how to determine the contour line of the fringe pattern and interfringe spacing. Several investigators [13–19] proposed various digital image-processing algorithms for extracting the contour line of the fringe patterns. This process can be classified into two manners. In the first one, the fringe field is identified as a binary image and the fringe skeletons are obtained using algorithms that were primarily developed for optical character recognition.

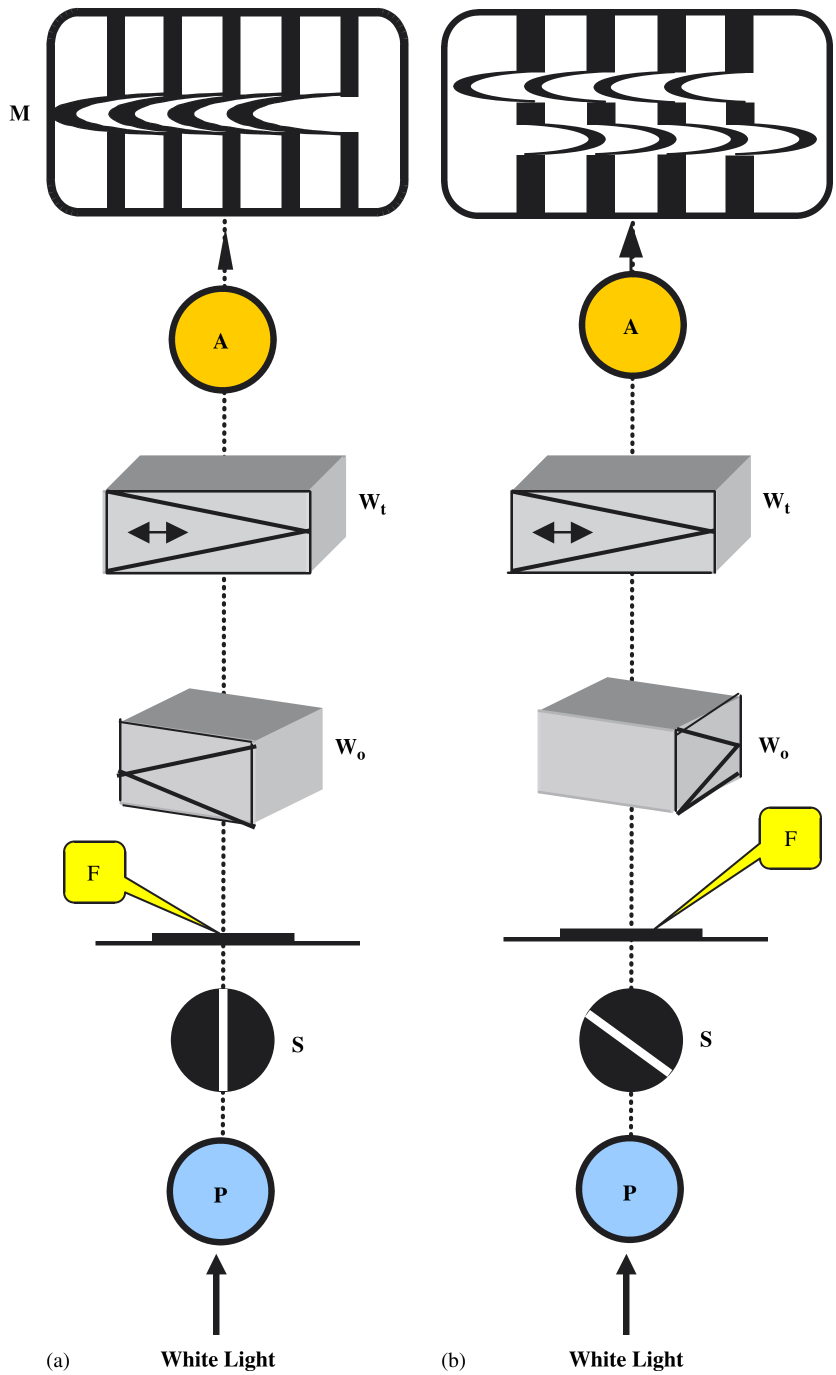

Fig. 1. Optical set up of Pluta interference microscopes in which; P polarizer, S slit diaphragm, F fibre, W_o and W_t Wollaston prisms, A analyser and M microinterferogram. Where (a) subtractive (non-duplicated) position and (b) Crossed (duplicated) position.

The algorithm applied by Hamza et al. [20] comes under this manner. In the second manner, the intensity variation within a fringe is used in devising algorithms for fringe skeleton determination. The algorithm applied by EL-Morsy et al. [21] comes under this manner.

Determination of the optical properties of fibres using double-beam interference fringes depends on calculating the fringe shift through the fibre and interfringe spacing in the liquid region. In fact, most of the authors used two-beam interference fringes to measure the fringe shift and the interfringe spacing manually. The main focus in this paper is the use of designed software to analyse the two-beam interference fringes pattern using Fourier transform technique for presenting an accurate measurement of the refractive indices ($n^{\parallel}$ & $n^{\perp}$), birefringence (Δn), and their profiles of fibres automatically (taking into consideration the refraction of the incident light inside the fibre).

2. Experimental technique

2.1. Two-beam interference Pluta microscope

The double refracting polarizing interference microscope designed, developed and applied by Pluta [1,2] is especially suitable for microinterferometry of birefringent fibres. This microscope is being used to carry out observations on various micro-objects that produce either a shift in the phase or in amplitude of light wave being transmitted. This microscope also serves the purpose of measuring the optical path difference (or phase shift), gradient of the optical path difference thickness, refractive index, birefringence and other physical quantities [1,2]. The setup of Pluta microscope [1,2] is shown in Fig. 1. It consists of two double refracting prisms W_o and W_t from the Wollaston type. One of these prisms W_o is installed in the microscope objective while the other W_t is positioned in the microscope tube. Using these two prisms, the microscope can work in two positions, which are the subtractive, and the crossed positions. The objective prism W_o is adjusted by rotation at its subtractive or crossed position with the main prism W_t. The crossed position (Fig. 1b) is applied to give the duplicated image (Fig. 2a) for measuring the refractive indices ($n^{\parallel}$ and $n^{\perp}$) of fibre, while the subtractive position (Fig. 1a) is applied to give the non-duplicated image (Fig. 2b) for measuring the birefringence (Δn) of fibre.

2.2. Automated two-beam interference Pluta microscope

The double-beam interference microscope is automated by attaching it to a computerized unit consists of; Panasonic CCD micro-camera, PC computer, digital frame grabber memory, and digital monitor. By which the microinterferogram (fibre image) is captured using CCD camera. This image is digitized directly via the digitizer frame grabber that built in the computer. The digitized image is recorded on the computer storage media. This recorded microinterferogram is analysed using Fourier transform method with software program prepared by us to calculate the refractive indices and birefringence of fibre.

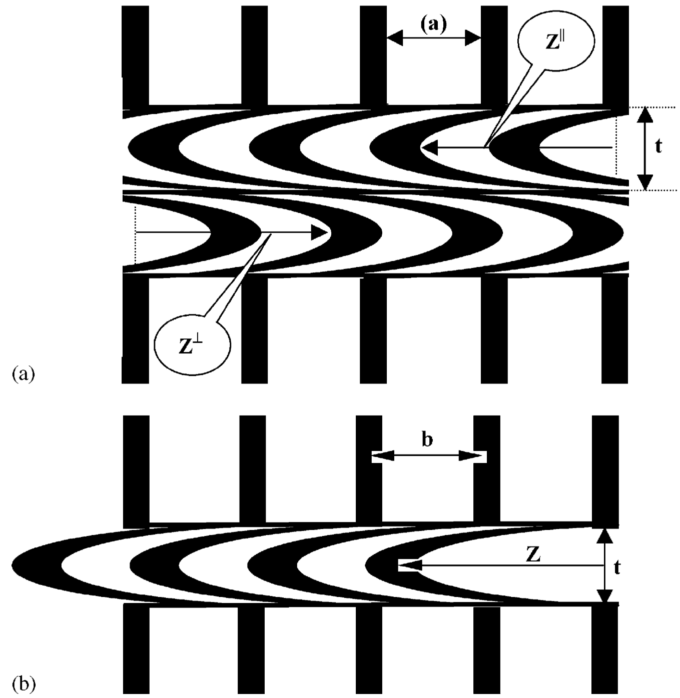

Fig. 2. Schematic diagram of the microinterferograms crossed by the fibre in two positions (a) duplicated and (b) non-duplicated, where $Z^{\parallel}$ and $Z^{\perp}$ are the fringe displacements in case of light vibrating parallel and perpendicular to the fibre axis, respectively, b is the interfringe spacing and t is the fibre thickness.

3. Theoretical considerations

3.1. Refractive indices ($n^{\parallel}$ and $n^{\perp}$) and birefringence Δn of fibres

Using the duplicated (Fig. 2a) image of the two-beam Pluta interference microscope, Barakat and Hamza [22] presented two methods, distance method and area method, for calculating the mean values of the fibre refractive indices in case of the light vibrating parallel and perpendicular ($n^{\parallel}$ and $n^{\perp}$) to the fibre axis. The two methods (distance and area) are represented, respectively, by the following equations [22]:

$$n^i = n_L \pm \frac{Z^i \lambda}{bt}, \quad (1)$$

$$n^i = n_L \pm \frac{F^i \lambda}{bA}, \quad (2)$$

where i denotes the state of light polarization $\parallel$ or $\perp$, n_L is the refractive index of the immersion liquid, Z is the fringe shift displacement, λ is the wavelength of the monochromatic light used, b is the interfringe spacing, t is the fibre thickness, F is the area enclosed under the fringe shift in the fibre and A is the cross-sectional area of the fibre. The area method (Eq. (2)) is applied for the fibres having regular and irregular cross-sections, but the distance method (Eq. (1)) is valid only in case of the regular cross-section fibres.

Using the non-duplicated image (Fig. 2(b)) produced by the polarizing interference microscope and the mentioned methods [22], the mean birefringence Δn of the fibre can be obtained directly from the following equations [23]:

$$\Delta n = \frac{Z\lambda}{bt} \quad \text{and} \quad \Delta n = \frac{F\lambda}{bA}. \tag{3}$$

Moreover, the birefringence can be calculated indirectly via the difference between the refractive indices $n^{\parallel}$ and $n^{\perp}$ from the duplicated microinterferogram.

3.2. *Refractive index and birefringence profile taking into consideration the refraction of light inside the fibre*

(I) Refractive index profile: The refractive index profile of a fibre reflects the variation of its refractive index across the fibre diameter. In case of the duplicated position of the interference Pluta microscope, the

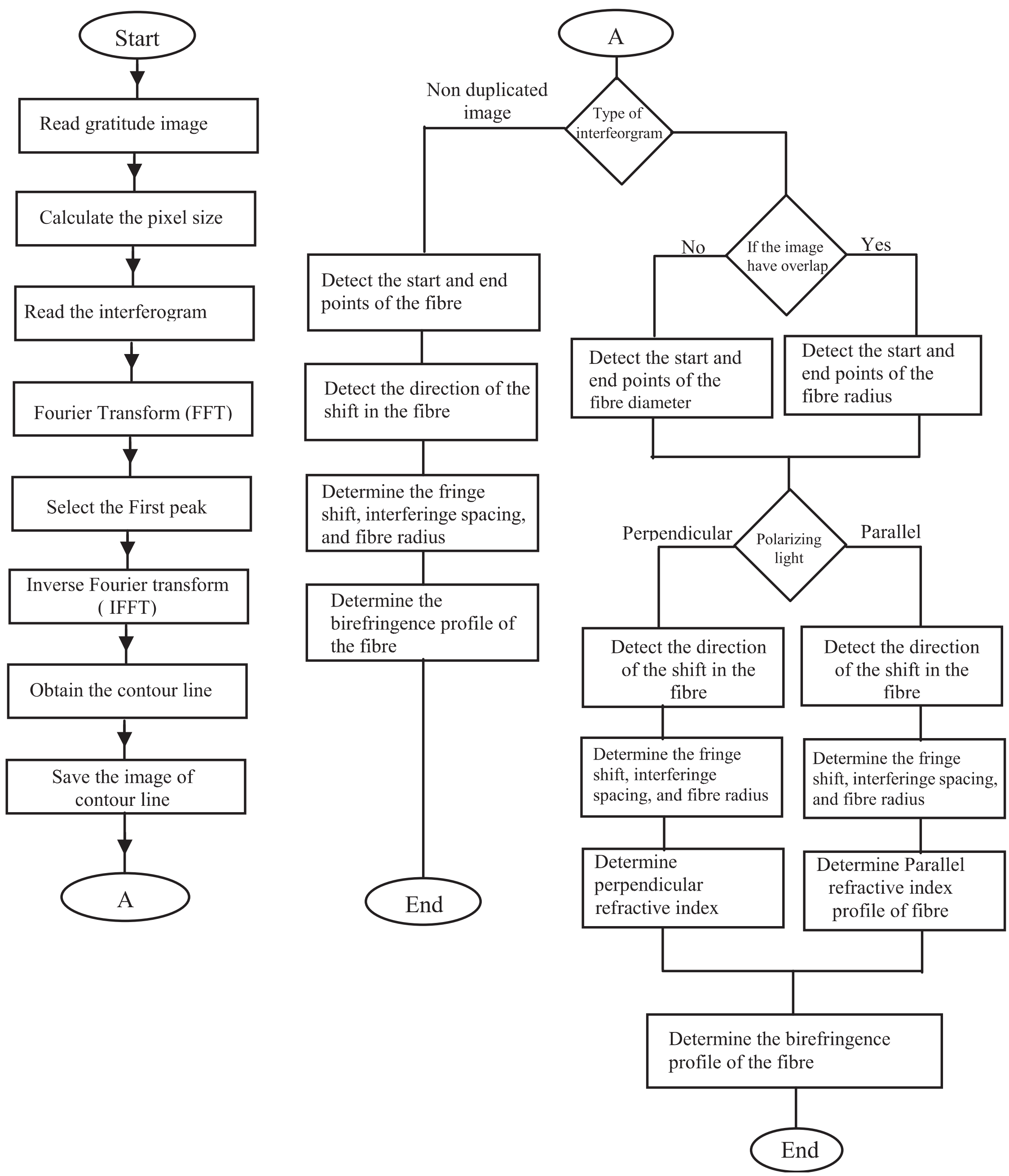

Fig. 3. The flow chart of the designed software program.

refractive index profile of fibres (taking into account the refraction of the incident beam by the fibre layers) can be obtained from the following equation [9]:

$$\frac{\lambda Z_Q}{b} = \sum_{j=1}^{Q-1} 2n_j[K1 - K2]^{1/2} + 2n_Q K3 - n_0 K4, \qquad (4)$$

where $K1$, $K2$, $K3$ and $K4$ are given by

$$K1 = \sqrt{[R-(j-1)a]^2 - (d_Q n_o/n_j)^2},$$

$$K2 = \sqrt{(R-ja)^2 - (d_Q n_o/n_j)^2},$$

$$K3 = \sqrt{[R-(Q-1)a]^2 - (d_Q n_o/n_Q)^2},$$

$$K4 = \sqrt{R^2 - d_Q^2} + \sqrt{R^2 - x_Q^2},$$

where a is the layer thickness ($a = R/N$), N is the number of layers, R is the fibre radius, Q is the layer number, d_Q is the distance between the incident and the fibre centre, X_Q is the distance between the emerging beam and the fibre centre, and Z_Q is the fringe shift corresponding to the point X_Q in the two-beam interference pattern.

(II) Birefringence profile: Usually most of authors use the duplicated image to determine the birefringence profile of a polymer fibre from the difference between the calculated refractive indices ($n^{\parallel}$ and $n^{\perp}$) profiles, for example see Ref. [24]. In this paper, using the non-duplicated image and substituting $n_o = 0$ in Eq. (4), we obtain the following set of equations:

For the first layer fibre,

$$\Delta n_1 = \frac{\lambda \Delta Z_1}{2Rb}. \qquad (5\text{-}1)$$

Table 1
Refractive indices ($n^{\parallel}$ and $n^{\perp}$) of basalt fibre

Refractive index	Distance method	Area method
$n^{\parallel}$	1.564	1.567
$n^{\perp}$	1.565	1.568

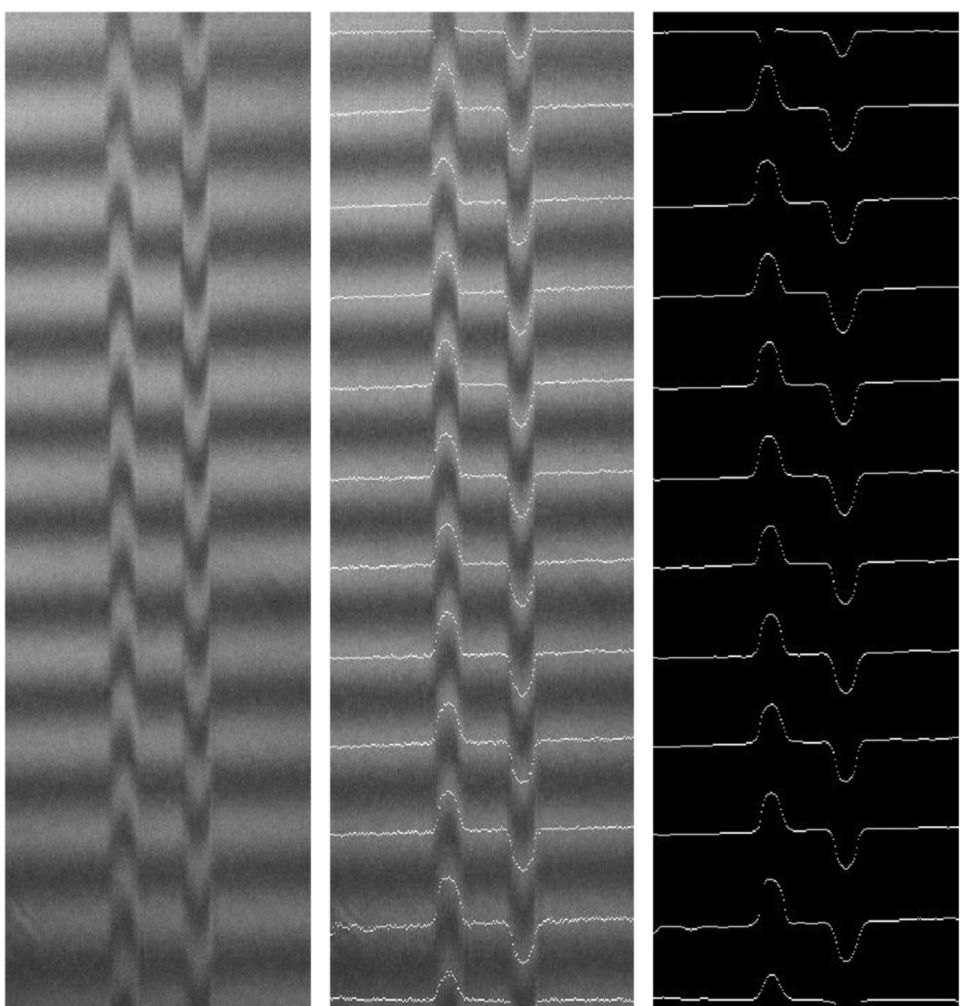

Fig. 4. The experimental duplicated microinterferogram of Basalt fibre using the automated Pluta interference microscope at monochromatic light of wavelength 546.1 nm where (a) original image, (b) original image with contour line, and (c) contour line image.

For the second layer fibre

$$\Delta n_2 = \left[\frac{1}{R-a}\right]\left[\frac{\lambda \Delta Z_2}{2b} - a\Delta n_1\right]. \qquad (5\text{-}2)$$

For the third layer fibre,

$$\Delta n_3 = \left[\frac{1}{R-2a}\right]\left[\frac{\lambda \Delta Z_3}{2b} - a(\Delta n_1 + \Delta n_2)\right]. \qquad (5\text{-}3)$$

Generally, for multi-layer fibre,

$$\Delta n_Q = \left[\frac{1}{R-(Q-1)a}\right]\left[\frac{\lambda \Delta Z_Q}{2b} - a\sum_{j=1}^{j=Q-1} \Delta n_j\right]. \qquad (6)$$

Therefore birefringence profile can be obtained, taking into account the refraction of the incident beam by the fibre layers, from the above Equation (6). As far as we know, this is the first time to calculate the birefringence profile from the non-duplicated image directly without the calculation of the refractive indices $n^{\parallel}$ and $n^{\perp}$.

A software program based on the given Equation (4) [9] and the derived Equation (6) is designed for automatic measurement of the refractive index and birefringence profiles. In this program, the contour line is obtained directly from the original microinterferogram by using the Fourier transform technique. The function of this program is described by the flow chart shown in Fig. 3.

4. Results and discussion

4.1. Refractive index profile of basalt fibre

Using the automated Pluta interference microscope, a sample of basalt fibres is immersed in a liquid of refractive index $n_L = 1.550$ and illuminated with a monochromatic light of wavelength $\lambda = 546.1$ nm. Then the interference fringe pattern (duplicated microinterferogram) is captured and recorded as shown in Fig. 4(a). Basalt sample is an isotropic and thin fibre, which gives a separated duplicated image of equal fringe shifts in the both directions as shown in Fig. 4(a). Using Fourier transform method with a software program prepared by ourselves, the original micro-interferogram (Fig. 4a) is contoured line in the both directions of polarization (∥ and ⊥ as shown in Fig. 4b). Fig. 4c shows the extracted fringe contour line on a dark background.

Entering the final contoured line microinterferogram (Fig. 4c) of basalt fibre as an input data to the designed software program, the fringe displacement Z, interfringe spacing b, fibre thickness t, the area enclosed under the fringe shift F, and the cross sectional area of the fibre A, are calculated automatically. Substituting by these parameters in Eqs. (1) and (2), the values of refractive indices ($n^{\parallel}$ and $n^{\perp}$) of basalt fibre are determined as given in Table 1.

The accuracy of the measured refractive indices using Pluta microscope (Wollaston prism), is about 0.05 λ and

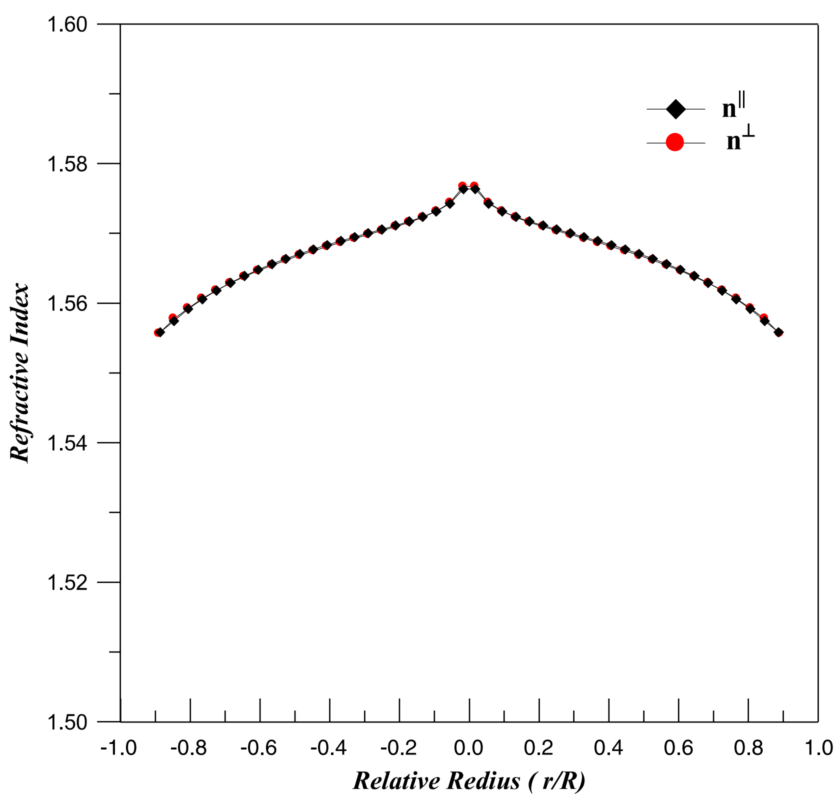

Fig. 5. The refractive index profiles of Basalt fibre at monochromatic light of wavelength 546 nm in case of light vibrating parallel and perpendicular to the fibre axis.

therefore the error in these values cannot be more than 0.003–0.001 [1,2].

The main purpose of our software is the calculation of refractive index profile taking into consideration the refraction of the incident light inside the fibre. The fringe shift profile was obtained from the microinterferograms (Fig. 4). Substituting into Eqs. (4) the refractive indices ($n^{\parallel}$ and $n^{\perp}$) of basalt fibre are computed across the fibre radius.

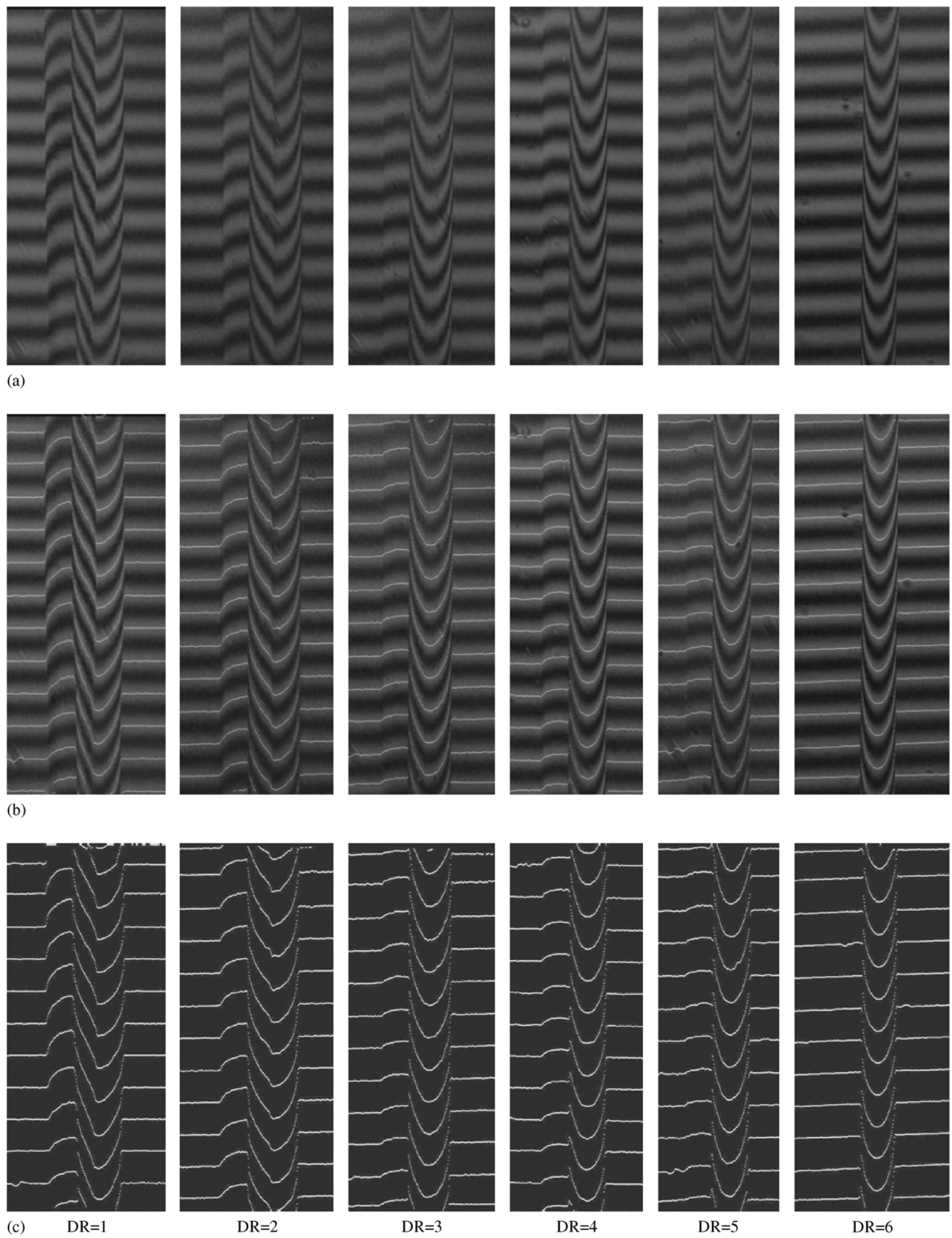

Fig. 6. The experimental duplicated microinterferogram of polypropylene fibres using the automated Pluta interference microscope at monochromatic light of wavelength 546 nm where (a) original image, (b) original image with contour line, and (c) contour line on dark background.

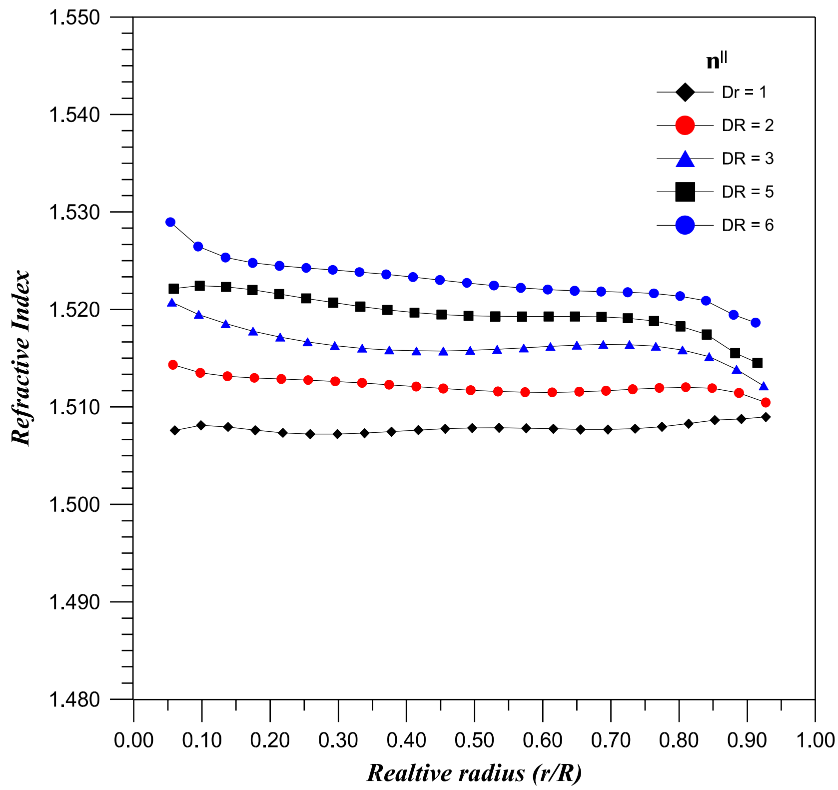

Fig. 7. Refractive index ($n^{\|}$) profiles of PP fibres at different draw ratios and monochromatic light of wavelength $\lambda = 546$ nm using automated Pluta microscope.

Fig. 5 shows the computed refractive index profiles (refractive index against the relative radius) of basalt fibre in which the values of refractive indices ($n^{\|}$ and $n^{\perp}$) are very close to each other and having the same behaviour across the fibre diameter. It is obvious from these profiles that, there is no difference between the refractive indices $n^{\|}$ and $n^{\perp}$ which means that the investigated sample (basalt fibre) is an isotropic or zero-birefringence fibre.

4.2. *Refractive index and birefringence profiles of polypropylene (PP) fibre at different draw ratios*

Automated Pluta microscope in its crossed position attached with the OTM drawing device [25] are applied to investigate a sample of PP fibres at different draw ratios (DR = 1, 2, 3, 4, 5, 6). The PP sample is anisotropic and thick fibre so it gives an overlapped duplicated image of unequal fringe shifts in both directions as shown in Fig. 6. Our software program is designed to overcome this difficulty. Fig. 6(a) shows the obtained duplicated micro-interferograms of PP fibres at different draw ratios using an immersion liquid $n_L = 1.497$ and monochromatic light of wavelength $\lambda = 546.1$ nm. Fig. 6b shows the contour lines traced inside the original pattern, while Fig. 6c shows the separated contour lines on the dark background.

The contour line microinterferograms of PP fibres (Fig. 6c) are entered into the software program, the refractive index profiles $n^{\|}$ and $n^{\perp}$ for PP fibre at different draw ratios and light of wavelength $\lambda = 546.1$ nm are obtained as given in Figs. 7 and 8, respectively. In these figures, the values of refractive indices are represented as a function of the relative radius of PP fibre. The effect of axial cold drawing on these fibres can be interpreted from the obtained profiles. It is clear that the increase of draw ratio results in an increase in the refractive index $n^{\|}$ and a decrease in the refractive index $n^{\perp}$.

Previously Hamza et al. [24] determined the birefringence profile of a polymer fibre via indirect method in which the values of birefringence were obtained from the difference between the calculated refractive indices ($n^{\|}$ and $n^{\perp}$) profiles. By the same manner and via the subtraction of the values of refractive index profile $n^{\perp}$ (Fig. 7) from that of $n^{\|}$ (Fig. 8), the birefringence profiles for PP fibres are manually calculated at different draw ratios as demonstrated in Fig. 9.

Now the automated interference Pluta microscope in its subtractive position is used to capture and record the non-duplicated microinterferograms of PP fibres at different draw ratios as illustrated in Fig. 10. Also Fig. 10 illustrates the contour line images of the obtained non-duplicated microinterferograms of PP fibres at different draw ratios. Using Eq. (6) and the non-duplicated contour line images (Fig. 10), the birefringence Δn profiles (taking into account the refraction of the incident light inside the fibre) for PP fibres are automatically calculated at different draw ratios as shown in Fig. 11.

Figs. 9 and 11 show the same behaviour for birefringence profiles of PP fibres, but there is a small difference

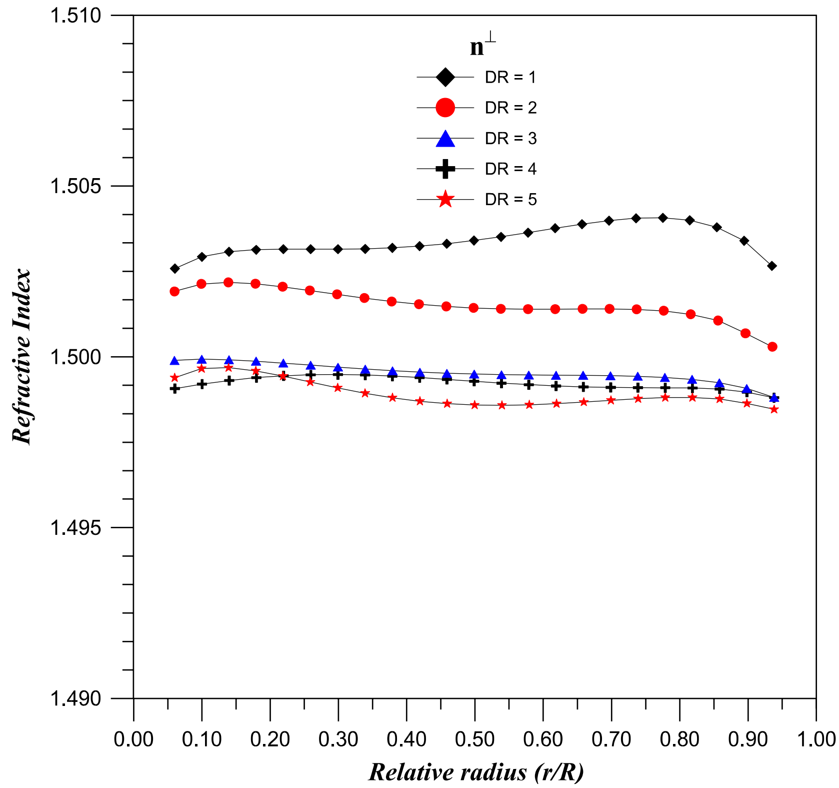

Fig. 8. Refractive index ($n^{\perp}$) profiles of PP fibres at different draw ratios and monochromatic light of wavelength $\lambda = 546\,\text{nm}$ using automated Pluta microscope.

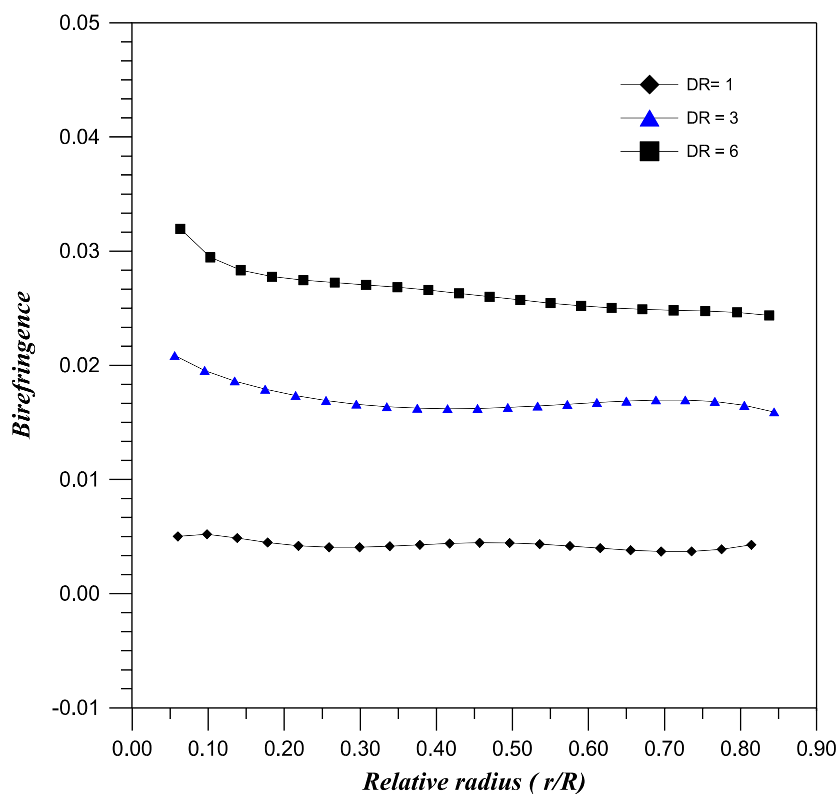

Fig. 9. Birefringence (Δn) profiles of PP fibres at different draw ratios by indirect method.

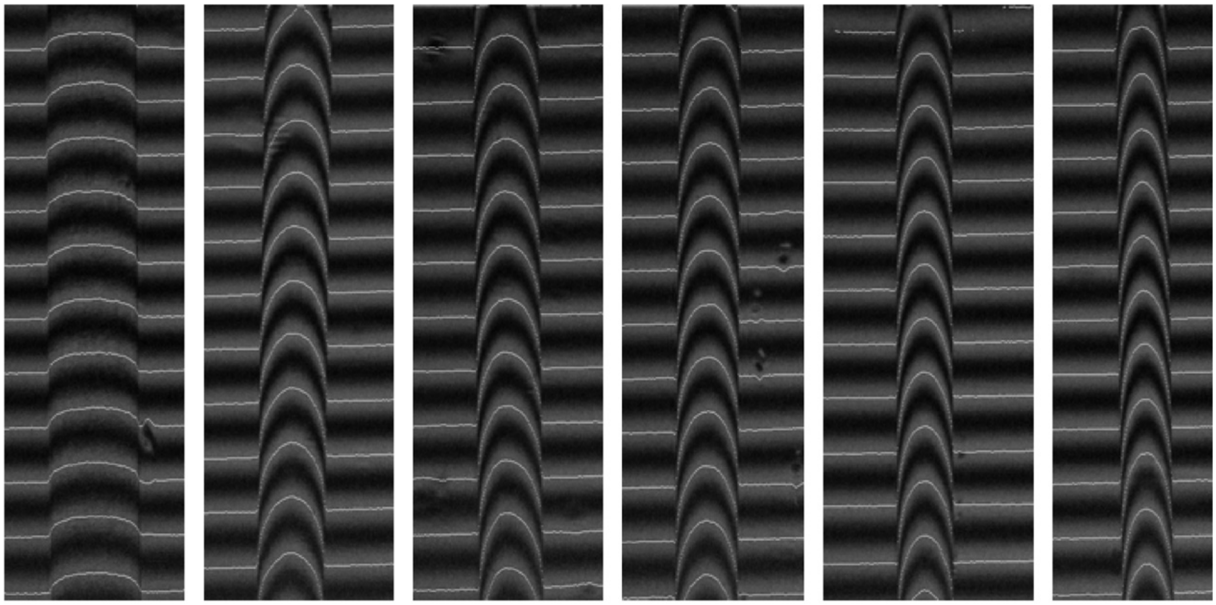

Fig. 10. The original non-duplicated experimental interferogram with contour line of polypropylene fibres using the automated Pluta interference microscope at monochromatic light of wavelength 546 nm with different draw ration (DR = 1, 2, 3, 4, 5, 6, respectively).

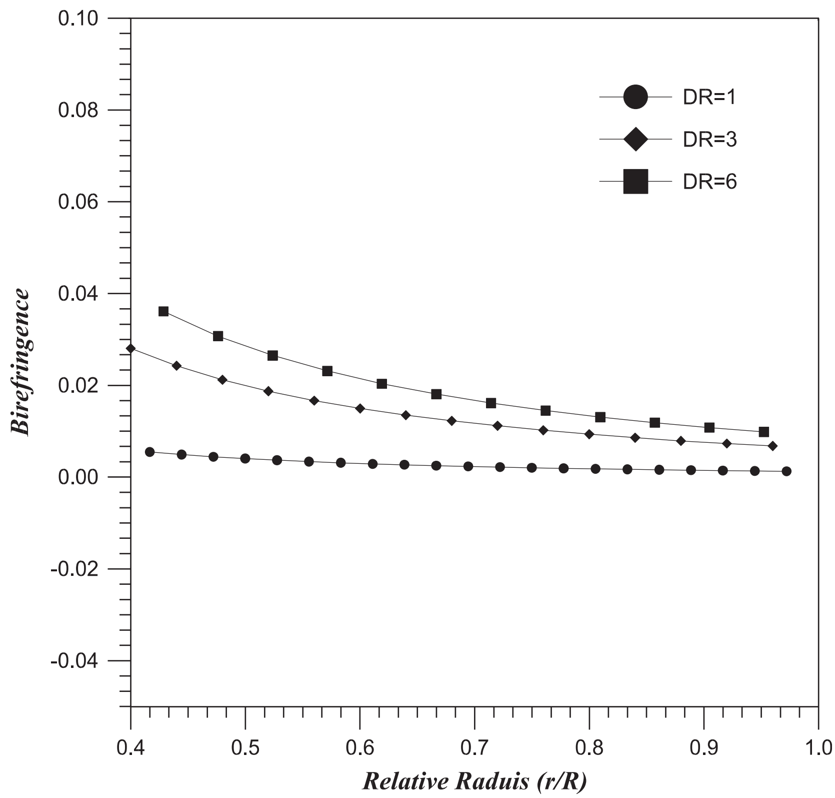

Fig. 11. Birefringence (Δn) profiles of PP fibres at different draw ratios and monochromatic light of wavelength $\lambda = 546$ nm using new (direct) method.

between their values, as shown in Fig. 12, due to the different methods of calculation (direct or indirect). The authors recommended the new (direct) method rather than the conventional (indirect) method. The error of the indirect method is twice of the new method. This is because the automated measurements in indirect method are obtained from two shifts (duplicated image), while in the direct method these measurements are obtained from a single shift (non-duplicated image).

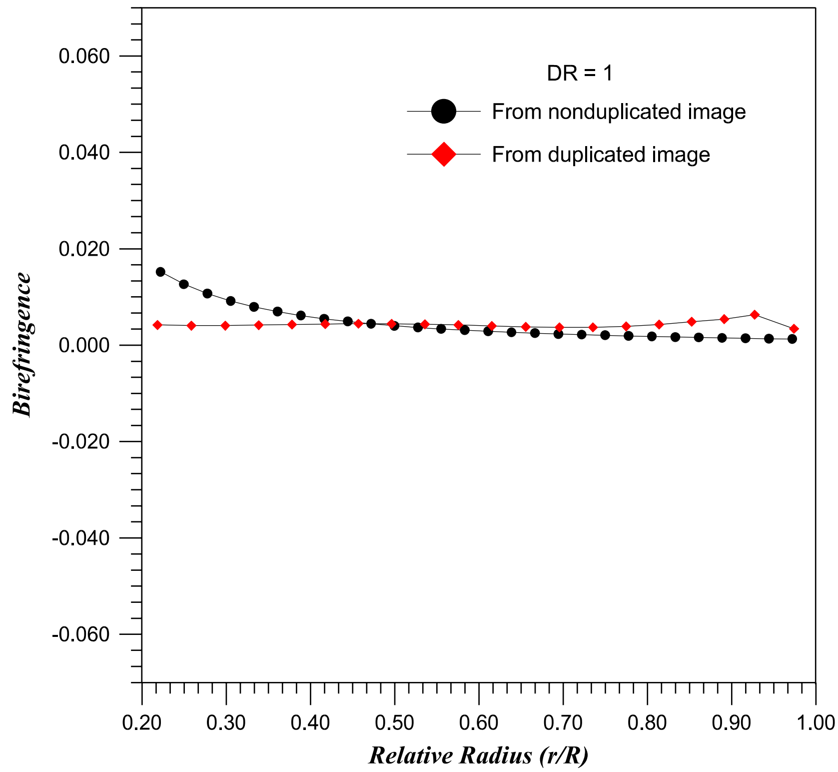

Fig. 12. Birefringence (Δn) profiles of PP fibres at DR = 1 and monochromatic light of wavelength $\lambda = 546$ nm using duplicated and non-duplicated interferogram.

5. Conclusion

The following points can be concluded:

1. The automated two-beam Pluta interference microscope and the designed software programs are accurate and quick technique for evaluating the optical properties of fibres.
2. The duplicated and non-duplicated microinterferograms of fibres using Pluta microscope are easily contoured and hence can be analysed automatically.
3. Based on the fringe pattern analysis of the duplicated (separated and overlapped) image, the refractive index profiles ($n^{||}$ and $n^{\perp}$) of fibres are determined.
4. Birefringence profile of fibres measured by the new (direct) method is recommended than that calculated by the conventional (indirect) method.
5. The change in the birefringence profile due to the cold drawing process for PP fibre is investigated automatically.

Acknowledgement

We would like to express our deep thanks to Prof. Dr. A.A. Hamza, for his encouragement, useful discussions, lending many facilities.

References

[1] Pluta M. Opt Acta 1971;18:661.
[2] Pluta M. J Microsc 1972;96:309.
[3] Marhic ME, Ho PS, Epstein M. Appl Phys Lett 1975;26:574.
[4] Saunders MJ, Gardner WB. App Opt 1977;16:2368.
[5] Barakat N, Hamza AA, Goneid AS. App Opt 1985;24.
[6] Sokkar TZN. Opt Commun 1991;35:187.
[7] Sokkar TZN. Appl Opt 1992;31:1229.
[8] Hamza AA, Ghander AM, Sokkar TZN, Mabrouk MA, Ramadan WA. Pure Appl Opt 1994;3:943.
[9] Hamza AA, Ghander AM, Sokkar TZN, Mabrouk MA, Ramadan WA. Pure Appl Opt 1995;4:161.
[10] Meanakshi M, Ravichandran VC. Photonics 96. International conference on fibre optic and photonics 1996;750.
[11] Sokkar TZN, Mabrouk MA, El-Bawab HF. J Opt A: Pure Appl Opt 1999;1:64.
[12] Gaur AH, De Vries H. J Polym Sci 1975;13:835.
[13] Nakadate S, Yatagai T, Saito H. Appl Opt 1983;22(2):237.
[14] Qifeng Yu, Andresen K. Appl Opt 1994;33(29):6873.
[15] Chen TY, Taylor CE. Exp Mech 1989;29:323.
[16] Ramesh K, Singh RK. Electron Imaging 1995;4:71.
[17] Yao JY. Exp Mech 1990;30:264.
[18] Yu QY, Liu XL, Sun X. Appl Opt 1998;37:4504.
[19] Eichhorn N, Osten W. J Mod Opt 1988;l35:1717.
[20] Hamza AA, Sokkar TZN, Mabrouk MA, El-Morsy MA. J Appl Polym Sci 2000;77:3099.
[21] ElMorsy MA, Yatagai T, Hamza AA, Mabrouk MA, Sokkar TZ. J Appl Polym Sci 2002;85(3):475–84.
[22] Hamza AA. Text Res J 1980;50:731.
[23] Simmens SC. Nature 1958;181:1260.
[24] Hamza AA, Sokkar TZN, El Farahaty KA, El Dessouky HM. J Opt A: Pure Appl Opt 1999;1:41.
[25] Hamza AA, Sokkar TZN, ElFarahaty KA, El Dessouky HM. J Appl Polym Sci 2005;95:647.